IJIRSET
International Journal of Innovative Research in
SCIENCE | ENGINEERING | TECHNOLOGY

e-ISSN: 2319-8753 | p-ISSN: 2347-6710

INTERNATIONAL JOURNAL OF INNOVATIVE RESEARCH

IN SCIENCE | ENGINEERING | TECHNOLOGY

Volume 12, Issue 7, July 2023

ISSN INTERNATIONAL STANDARD SERIAL NUMBER INDIA

Impact Factor: 8.423

9940 572 462 | 6381 907 438 | ijirset@gmail.com | www.ijirset.com

International Journal of Innovative Research in Science, Engineering and Technology (IJIRSET)

|e-ISSN: 2319-8753, p-ISSN: 2320-6710| www.ijirset.com | Impact Factor: 8.423| A Monthly Peer Reviewed & Referred Journal |

|| Volume 12, Issue 7, July 2023 ||

| DOI:10.15680/IJIRSET.2023.12070010|

Computational Fluid Dynamics Analysis of Shell and Tube Heat Exchanger

Aviral Verma[1], Dr. Nitin Tenguria[2]

Research Scholar, Department of Mechanical, Sagar Institute of Research and Technology, Bhopal, India[1]

Head of Dept., Department of Mechanical, Sagar Institute of Research and Technology, Bhopal, India[2]

ABSTRACT:- Three-dimensional CFD simulations are carried out to investigate heat transfer and fluid flow characteristics of a two-row plain fin-and-tube heat exchanger using ANSYS FLUENT. Heat transfer and pressure drop characteristics of the heat exchanger are investigated for Reynolds numbers ranging from 330 to 7200. Model geometry is created, meshed, calculated, and post-processed using ANSYS Workbench. Fluid flow and heat transfer are simulated and results compared using both laminar and turbulent flow models (k-epsilon, and SST k-omega), with steady-state solvers to calculate pressure drop, flow, and temperature fields. Model validation is carried out by comparing the simulated case friction factor f and Colburn j factor with experimental results from the literature. Reasonable agreement is found between the simulations and experimental data, and the ANSYS FLUENT software has been sufficient for simulating the flow fields in tube-fin heat exchangers.

KEYWORDS: Ansys Fluent, Heat Exchange, CFD, k-epsilon turbulence model, simulating laminar flow

I. INTRODUCTION

Fin-and-tube heat exchangers are widely-used heat transfer devices in applications like refrigeration and air conditioning systems. It's easier manufacturing, simpler construction, lower cost, and relatively easy in maintenance makes it one of the most commonly used heat exchangers. They can be applicable to both heating and cooling. Once the cooling process takes place below dew point temperature, condensate forms on the surface and result in a complex heat and mass transfer interactions.

A heat exchanger is a system used to transfer heat between two or more fluids. Heat exchangers are used in both cooling and heating processes. The fluids may be separated by a solid wall to prevent mixing or they may be in direct contact. They are widely used in space heating, refrigeration, air conditioning, power stations, chemical plants, petrochemical plants, petroleum refineries, natural-gas processing, and sewage treatment. The classic example of a heat exchanger is found in an internal combustion engine in which a circulating fluid known as engine coolant flows through radiator coils and air flows past the coils, which cools the coolant and heats the incoming air. Another example is the heat sink, which is a passive heat exchanger that transfers the heat generated by an electronic or a mechanical device to a fluid medium, often air or a liquid coolant.

Flow Arrangement

There are three primary classifications of heat exchangers according to their flow arrangement. In parallel-flow heat exchangers, the two fluids enter the exchanger at the same end, and travel in parallel to one another to the other side. In counter-flow heat exchangers the fluids enter the exchanger from opposite ends. The counter current design is the most efficient, in that it can transfer the most heat from the heat (transfer) medium per unit mass due to the fact that the average temperature difference along any unit length is higher. In a cross-flow heat exchanger, the fluids travel roughly perpendicular to one another through the exchanger.

For efficiency, heat exchangers are designed to maximize the surface area of the wall between the two fluids, while minimizing resistance to fluid flow through the exchanger. The exchanger's performance can also be affected by the addition of fins or corrugations in one or both directions, which increase surface area and may channel fluid flow or induce turbulence. The driving temperature across the heat transfer surface varies with position, but an appropriate mean temperature can be defined. In most simple systems this is the "log mean temperature difference" (LMTD).

|e-ISSN: 2319-8753, p-ISSN: 2320-6710| www.ijirset.com | Impact Factor: 8.423| A Monthly Peer Reviewed & Referred Journal |

|| Volume 12, Issue 7, July 2023 ||

| DOI:10.15680/IJIRSET.2023.12070010|

Types of Heat Exchangers

Shell and Tube Heat Exchanger

Shell and tube heat exchangers consist of a series of tubes which contain fluid that must be either heated or cooled. A second fluid runs over the tubes that are being heated or cooled so that it can either provide the heat or absorb the heat required.

Several thermal design features must be considered when designing the tubes in the shell and tube heat exchangers: There can be many variations on the shell and tube design. Typically, the ends of each tube are connected to plenums (sometimes called water boxes) through holes in tubesheets. The tubes may be straight or bent in the shape of a U, called U-tubes.

- Tube diameter: Using a small tube diameter makes the heat exchanger both economical and compact. However, it is more likely for the heat exchanger to foul up faster and the small size makes mechanical cleaning of the fouling difficult. To prevail over the fouling and cleaning problems, larger tube diameters can be used. Thus to determine the tube diameter, the available space, cost and fouling nature of the fluids must be considered.
- Tube length: heat exchangers are usually cheaper when they have a smaller shell diameter and a long tube length. Thus, typically there is an aim to make the heat exchanger as long as physically possible whilst not exceeding production capabilities. However, there are many limitations for this, including space available at the installation site and the need to ensure tubes are available in lengths that are twice the required length (so they can be withdrawn and replaced). Also, long, thin tubes are difficult to take out and replace.

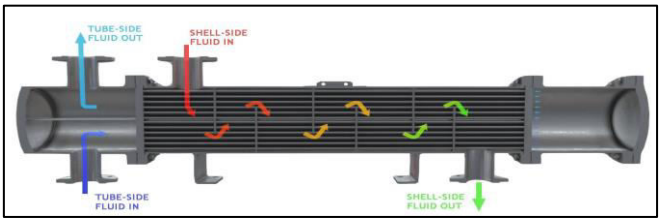

Fig 1.1 Shell and Heat Tube Exchanger

Plate Heat Exchangers

Another type of heat exchanger is the plate heat exchanger. These exchangers are composed of many thin, slightly separated plates that have very large surface areas and small fluid flow passages for heat transfer. Advances in gasket and brazing technology have made the plate-type heat exchanger increasingly practical. In HVAC applications, large heat exchangers of this type are called *plate-and-frame*; when used in open loops, these heat exchangers are normally of the gasket type to allow periodic disassembly, cleaning, and inspection. There are many types of permanently bonded plate heat exchangers, such as dip-brazed, vacuum-brazed, and welded plate varieties, and they are often specified for closed-loop applications such as refrigeration. Plate heat exchangers also differ in the types of plates that are used, and in the configurations of those plates. Some plates may be stamped with "chevron", dimpled, or other patterns, where others may have machined fins and/or grooves.

When compared to shell and tube exchangers, the stacked-plate arrangement typically has lower volume and cost. Another difference between the two is that plate exchangers typically serve low to medium pressure fluids, compared to medium and high pressures of shell and tube. A third and important difference is that plate exchangers employ more countercurrent flow rather than cross current flow, which allows lower approach temperature differences, high temperature changes, and increased efficiencies.

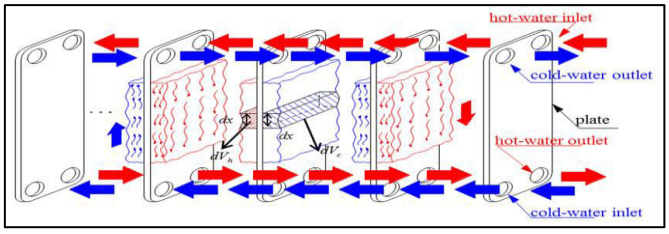

Fig 1.2 Plate Heat Exchangers

|e-ISSN: 2319-8753, p-ISSN: 2320-6710| www.ijirset.com | Impact Factor: 8.423| A Monthly Peer Reviewed & Referred Journal |

|| Volume 12, Issue 7, July 2023 ||

| DOI:10.15680/IJIRSET.2023.12070010|

Plate and shell heat exchanger

A third type of heat exchanger is a plate and shell heat exchanger, which combines plate heat exchanger with shell and tube heat exchanger technologies. The heart of the heat exchanger contains a fully welded circular plate pack made by pressing and cutting round plates and welding them together. Nozzles carry flow in and out of the platepack (the 'Plate side' flowpath). The fully welded platepack is assembled into an outer shell that creates a second flowpath (the 'Shell side'). Plate and shell technology offers high heat transfer, high pressure, high operating temperature, compact size, low fouling and close approach temperature. In particular, it does completely without gaskets, which provides security against leakage at high pressures and temperatures.

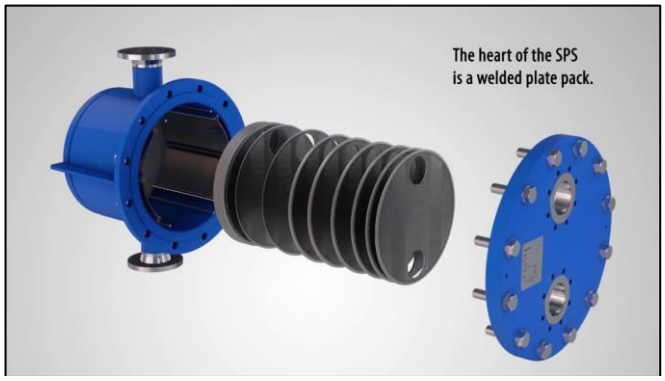

Fig 1.3 Plate and Shell Heat Exchanger

Adiabatic wheel heat exchanger

A fourth type of heat exchanger uses an intermediate fluid or solid store to hold heat, which is then moved to the other side of the heat exchanger to be released. Two examples of this are adiabatic wheels, which consist of a large wheel with fine threads rotating through the hot and cold fluids, and fluid heat exchangers.

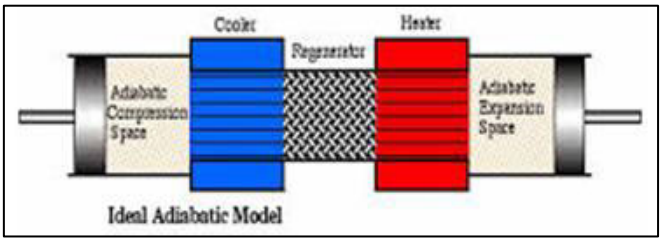

Fig 1.4 Adiabatic Wheel Heat Exchanger

II. MODEL DESCRIPTION

When fluids, surfaces, or combinations of these are at different temperatures and in thermal contact, heat exchangers are used to transfer thermal energy. Heat recovery, pasteurisation, distillation, and the heating or cooling of a specific fluid stream are examples of typical applications. A wall might divide the fluids or they can be in close touch. Appendages, or fins, can be connected to a wall acting as a heat transfer surface separating fluid in order to improve the heat transfer surface area.

Table 2.1 Geometrical Description

Geometric Parameter	Symbol	Dimensions
Fin Thickness	t	0.130 mm
Fin Pitch	Fp	2.240 mm
Fin collar Outside Diameter	Dc	10.23 mm
Transverse Pitch	Pt	25.40 mm
Longitudinal Pitch	Pl	22.00 mm
Tube Wall Thickness	δ	0.336 mm
Number of Tube Rows		2

|e-ISSN: 2319-8753, p-ISSN: 2320-6710| www.ijirset.com | Impact Factor: 8.423| A Monthly Peer Reviewed & Referred Journal |

|| Volume 12, Issue 7, July 2023 ||

| DOI:10.15680/IJIRSET.2023.12070010|

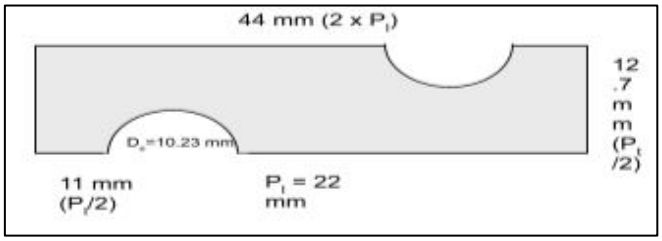

Fig 2.1 The primary computational domain and geometric parameters of the heat exchanger model under consideration are depicted in this diagram

The computational domain is specified by 0 x 8Pl, 0 y Pt/2, and 0 z Fp, and is 8 times the original heat transfer area (as shown in Figure 2.1), while the actual modelled heat exchanger length is equal to twice the longitudinal pitch Pl. To decrease oscillations and assure a representative flow in the computational domain of the actual heat exchanger, the volume representing the air that travels through the gap between the two fins is enlarged upstream from the inlet and downstream from the outlet.

Boundary Condition

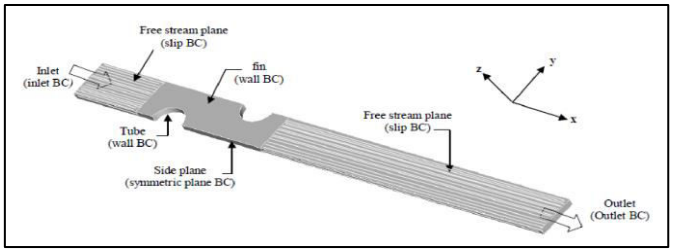

Fig 2.2 Boundary conditions (BC) and extended flow volumes are included in the computational domain.

Boundary conditions are present in the computational domain, as shown in Figure 2.2, with the following conditions:
Tube surfaces, Dirichlet BC:
$T = T_w$,
Air velocity: $u = v = w = 0$
Inlet, Dirichlet BC:
Uniform velocity $u = u_{in}$,
$v = w = 0$
$T = 5$ ℃.
Outlet, Neumann BC:
Zero gradients, u, v, w, pressure, and temperature. (One-way),
Free stream planes: (top and bottom planes of the extended surface areas):
'Slip' conditions: $(\partial u/\partial z) = 0$, $(\partial v/\partial z) = 0$, $w = 0$, $(\partial T/\partial z) = 0$.
Side planes: symmetry planes
$(\partial u/\partial y) = 0$, $v = 0$, $(\partial w/\partial y) = 0$, $(\partial T/\partial y) = 0$
The total computational domain was made up of 150521 finite volumes, with a structured grid running across most of it and an unstructured grid around the tubes. Based on the results of a grid independence test, the cell number was decided.

Numerical Mesh

The ANSYS Workbench design modeller is used to construct the geometry of the computational domain, and the Workbench mesh tool is used to create the mesh. Grid independence studies were conducted using both tetrahedral and hexagonal meshes to determine the optimal amount of cells to use in the mesh. This section explains how to create the geometry and meshes for this project in general.

Tetrahedral mesh

In the design modeller, geometry module of ANSYS workbench, the first heat exchanger geometry was developed. The mesh module was then utilised to make tetrahedral and hexahedral cells. Figures 2.3 depict the computational geometry and a mesh of 44199 tetrahedral cells, respectively.

|e-ISSN: 2319-8753, p-ISSN: 2320-6710| www.ijirset.com | Impact Factor: 8.423| A Monthly Peer Reviewed & Referred Journal |

|| Volume 12, Issue 7, July 2023 ||

| DOI:10.15680/IJIRSET.2023.12070010|

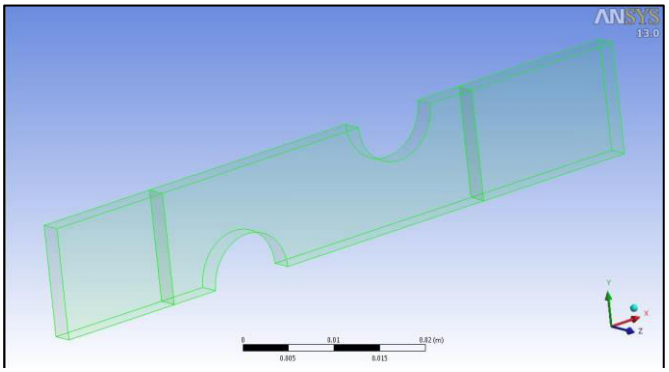

Fig 2.3 Actual Computational Geometry with extended domain

The tetrahedral mesh is unstructured, having finer mesh around the curved portions of the tubes, as shown in figure 2.4. Larger cells in the extended volume (not visible in image) reduce computation time. The thickness of geometry prevents the creation of more than three layers of cells (Z direction).

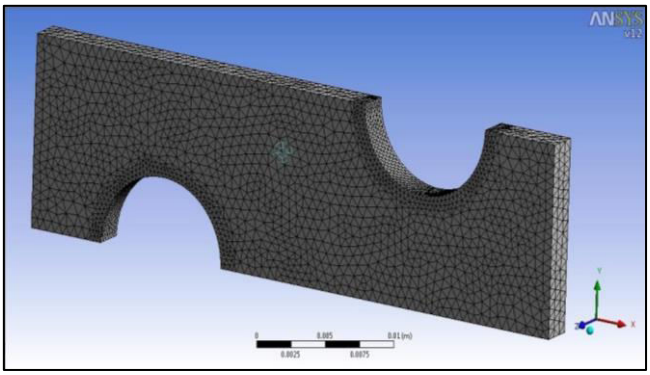

Fig 2.4 Tetrahedral mesh with 44199 elements

Hexagonal Mesh

Following the formation of the tetrahedral mesh, it was decided that a more structured grid would be preferable, as it is the most often used and known to deliver reliable computations. It was also recognized that having the capacity to create varied boundary conditions for the expanded volume, as opposed to the actual heat exchanger core to be emulated, was critical. As a result, the free flow air entering the core's inlet (and exit) has the correct boundary conditions (temperature and x-direction velocity) and is not required to have the same circumstances as the heat exchanger, resulting in less accurate simulations.

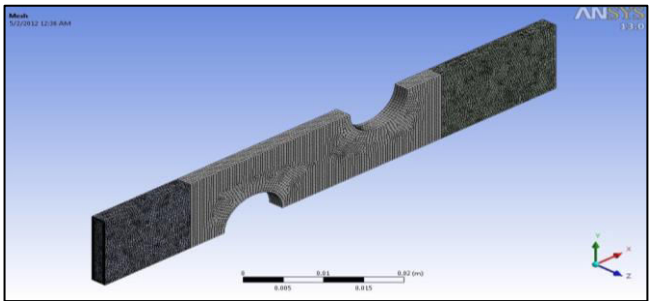

Fig 2.5 CFD computational domain for heat exchanger simulation

Governing Equations and Numerical Schemes

The three-dimensional continuity, Navier-Stokes for momentum and energy, and scalar transport equations for steady-state flow are the governing equations for this project, and they can be stated (usually) as follows:

Equation of Continuity:

|e-ISSN: 2319-8753, p-ISSN: 2320-6710| www.ijirset.com | Impact Factor: 8.423| A Monthly Peer Reviewed & Referred Journal |

|| Volume 12, Issue 7, July 2023 ||

| DOI:10.15680/IJIRSET.2023.12070010|

$$\frac{\partial(\rho u_i)}{\partial x_i} = 0. \quad (1)$$

Momentum equation:

$$\frac{\partial}{\partial x_i}(\rho u_i u_j) = \frac{\partial}{\partial x_i}\left(\mu \frac{\partial u_j}{\partial x_i}\right) - \frac{\partial p}{\partial x_j}. \quad (2)$$

Energy Equation:

$$\frac{\partial}{\partial x_i}(\rho u_i T) = \frac{\partial}{\partial x_i}\left(\frac{k}{C_p}\frac{\partial u_j}{\partial x_i}\right). \quad (3)$$

General Transport Equations (for scalers):

$$\frac{\partial(\rho u_i \phi)}{\partial x_i} = \frac{\partial}{\partial x_i}\left[\Gamma_\phi \frac{\partial \phi}{\partial x_i}\right] + S_\phi \quad (4)$$

In CFD calculations, the general equations 1-3 are used to determine the flow field for both thermal and fluid (air) dynamics, including heat transfer and pressure drop. The finite volume approach is used to discretize and solve them. It's solved on a staggered grid with laminar and turbulent flow solvers, with the latter using the Reynolds Averaged Navier-Stokes equations (RANS) with both k-epsilon and SST k-omega turbulence models. The SIMPLE algorithm is used to assure velocity and pressure coupling.

III. RESULTS AND DISCUSSION

Grid Independence Test

The grid independence test is performed to see how the size of the grid impacts simulation results. The same geometric model is simulated with different grid sizes in this test. As an independent grid, we employ a mesh that has no effect on the simulation output. This is to reduce the inaccuracy caused by the grid size (discretisation error). For this project, pressure loss between inlet and outlet is simulated using 5 mesh sizes with 1360, 32850, 44199, 150521, and 275324 cells. Based on the comparison of simulated results, the grid of 150521 cells is chosen as the independent grid size for the project. Despite the fact that mesh sizes with 150521 and 275324 cells produce virtually identical results, the one with 150521 cells takes less time to compute.

EXPERIMENTAL RESULTS

Experimental Values for Colburn j-Factor

Table 3.1 Experimental values for Colburn j- factor

Re	Colburn j factor
330	0.042
600	0.027
790	0.023
1300	0.017
1700	0.014
2900	0.012
4300	0.0094
5200	0.009
6200	0.0084
7200	0.0081

The Colburn j-factor decreases with increasing Reynolds number, as shown in Table 3.1 and Figure 3.1. The Reynolds number ranges from 0.042 at the lowest to 0.0081 at the highest. This graph for air flow through a heat exchanger has a more distinct dip in the transition region than a plot of this sort (j vs. Re) for a standard circular tube. However, at Reynolds number 1300, the graph appears to level off, and at Reynolds number 2900, the graph looks to level off again. As a result of this graph, it can be deduced that the laminar flow region extends up to roughly Reynolds number 1300

|e-ISSN: 2319-8753, p-ISSN: 2320-6710| www.ijirset.com | Impact Factor: 8.423| A Monthly Peer Reviewed & Referred Journal |

|| Volume 12, Issue 7, July 2023 ||

| DOI:10.15680/IJIRSET.2023.12070010|

(precise values are impossible to determine without more data points), there is a transition phase after that, and turbulent flow begins at around Reynolds number 2900. These experimental data are compared to values for the Colburn j-factor derived from simulations and followed by the required calculations for this project. The uncertainties in the Colburn j-factor values (experimentally derived values) can be considerable at the lower Reynolds numbers (uncertainty is 9.4% at Reynolds number 600, and may be much higher at Reynolds number 330, the value of which was not mentioned in the text).

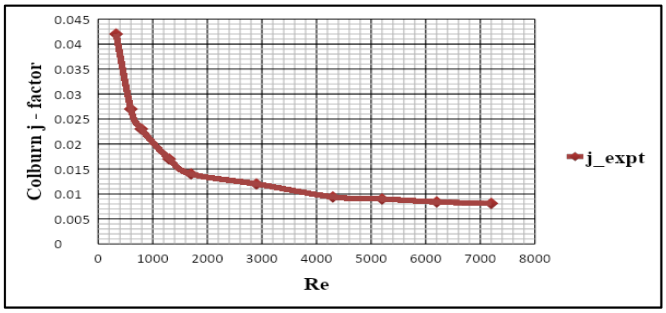

Fig 3.1 Plot of Reynolds Number Vs Colburn j- factor, determined experimentally

Experimental Values for Fanning Friction Factor f

The values for Reynolds number and friction factor f as read from the graph in the article for the specific heat exchanger shape explored in this project.

Table 3.2 Experimental values for Fanning friction factor f

Re	Friction factor f
330	0.11
600	0.073
790	0.063
1300	0.046
1700	0.042
2900	0.033
4300	0.027
5200	0.024
6200	0.022
7200	0.021

The Colburn j-factor, the Fanning friction factor f also decreases as the Reynolds number increases. It ranges from 0.11 at the lowest Reynolds number to 0.021 at the high Reynolds number. A slight change can be seen at Between Reynolds numbers 1300 and 1700, the graph levels off again. The laminar flow region appears to begin about Reynolds number 1300, with a transition region following, and the turbulent flow regime appears to begin at roughly Reynolds number 1700, based on the tiny change in the graph (or possibly it is closer to 2900 since that is what was found on the j-factor graph). More data points, on the other hand, would be required to precisely identify the critical Reynolds values for the various flow regimes. The uncertainties in the Fanning friction factor f values (experimentally determined values) can be large at the lower Reynolds numbers (the uncertainty is given as 17.7% at Reynolds number 600, and may be much higher for Reynolds number 330, the value of which was not provided in the text).

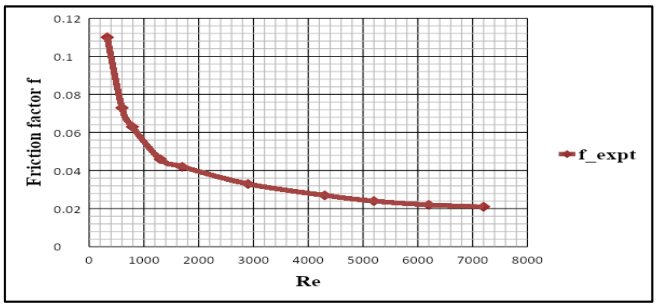

Fig 3.2 Plot of Reynolds Number Vs Fanning friction factor f, determined experimentally

|e-ISSN: 2319-8753, p-ISSN: 2320-6710| www.ijirset.com | Impact Factor: 8.423| A Monthly Peer Reviewed & Referred Journal |

|| Volume 12, Issue 7, July 2023 ||

| DOI:10.15680/IJIRSET.2023.12070010|

Numerical Results

Characteristics of Flow

After conducting the CFD simulations in ANSY Fluent, this part describes the observations made with CFD Post. With contour plots of velocity with vectors, the features of low-Reynolds flow and high-Reynolds flow are contrasted.

Observations of Velocity

The flow patterns of the two examples (inlet air velocity 0.3 m/s vs. 6.2 m/s) are comparable at low and high Reynolds numbers. The air enters from the left-hand inlet, flows in the direction of the arrows, and escapes out the right-hand outlet.

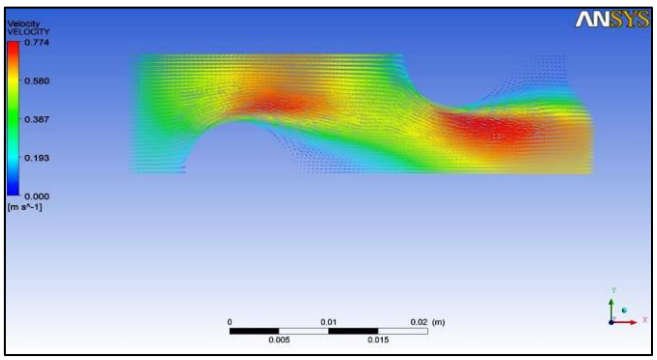

Fig 3.3 Velocity vector for inlet velocity 0.3 m/s, SST k-omega flow model

The air speeds up as it goes through the first tube in both cases, then speeds up again as it passes through the second tube. As indicated by the samples taken in the case files for average velocities at the minimal free-flow zones, the velocity flowing around the second tube is faster than the velocity flowing around the first tube. The minimum free-flow area is the area of the heat exchanger between two transverse tubes, so the area directly above tube one or just below tube two is the minimum free-flow area. In the air flow channel, the tubes work as a type of pipe constriction, forcing the flow to accelerate.

The areas with the highest velocity are just off the streamlines that travel directly around the tubes, and are in the least free-flowing area. In the instance of a 0.3 m/s inlet velocity, the top velocity at the second tube is 0.77 m/s, or roughly 2.5 times the inlet velocity. For the 6.2 m/s inlet flow example, the greatest velocity is 14.55 m/s, which is more than twice the intake velocity.

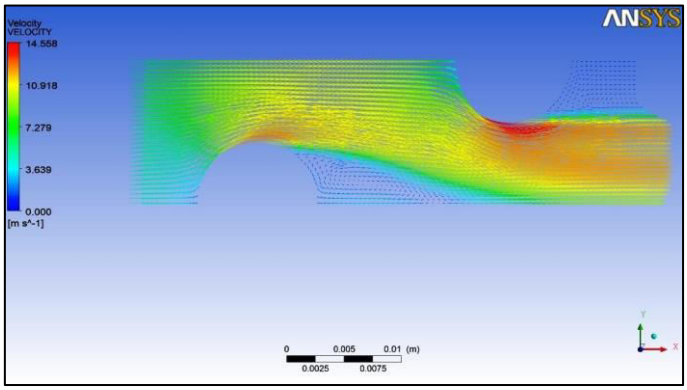

Fig 3.4 Velocity vector for inlet velocity 6.2 m/s, SST k-omega flow model

The size of the tubes has an effect on the Reynolds number of the air flowing around them, because with larger tubes (at the same distance from each other), the minimum free-flow area would be even smaller if the transverse pitch stayed the same. The tube collar diameter is used as the characteristic length for the Reynolds number in this study, and it can be observed that increasing this parameter (while keeping transverse pitch constant) can result in increased velocities, turbulence, and Reynolds number.

The recirculation zones behind each tube have tiny overflow areas in the case of greater air flow. The second recirculation zone looks to be greater than the first. A recirculation zone was not visible in the instance with a 0.3 m/s inlet velocity, as it was in the case with a 6.2 m/s inlet velocity.

|e-ISSN: 2319-8753, p-ISSN: 2320-6710| www.ijirset.com | Impact Factor: 8.423| A Monthly Peer Reviewed & Referred Journal |

|| Volume 12, Issue 7, July 2023 ||

| DOI:10.15680/IJIRSET.2023.12070010|

Characteristics of Heat Transfer

Figures 3.5 and 3.6 show contours indicating local temperature distributions for the identical instances as in the previous section. The first and most obvious difference between the two Reynolds number heat transfer characteristics is that once steady-state is established, the slower-moving air (0.3 m/s) gets heated up much more in the first two rows than higher Reynolds number flows. This must be because the air moves slowly enough that the heat has more time to absorb (a longer'residence time'). If the inlet conditions were set cyclical at the start, comparisons might be conducted farther down the heat exchanger (for example, after 10 or 12 rows) to see how the heat transfer compares.

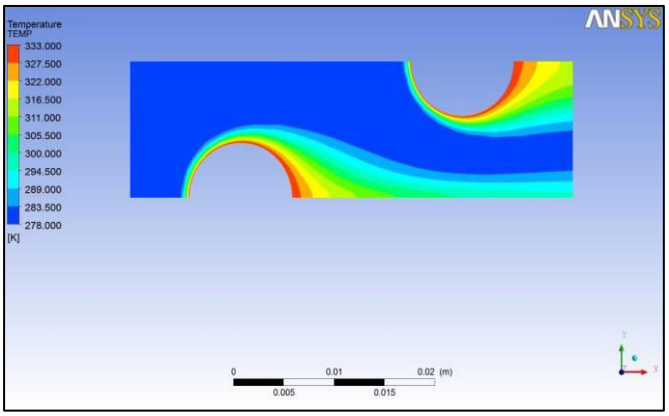

Figure 3.5 Contour of Temperature for inlet velocity 0.3 m/s, SST k-omega flow model

Figure 3.6 shows that the higher Reynolds number flow has a different pattern than the preceding example, as well as a lower temperature change (different kinds of isothermal streamlines). The highest temperature increases in this scenario occur shortly after each of the tubes in the recirculation and 'slow velocity' zones (seen before in the velocity vector plot). The slow-moving regions of the heat exchanger, like the slow-moving flow in the case of 0.3 m/s velocity, are likewise better able to absorb heat. The staggered tube system is designed to have these slower-moving and recirculation areas to keep the heat flowing to the air while also preventing recirculation zones from 'stagnating,' as can happen in inline arrangements.

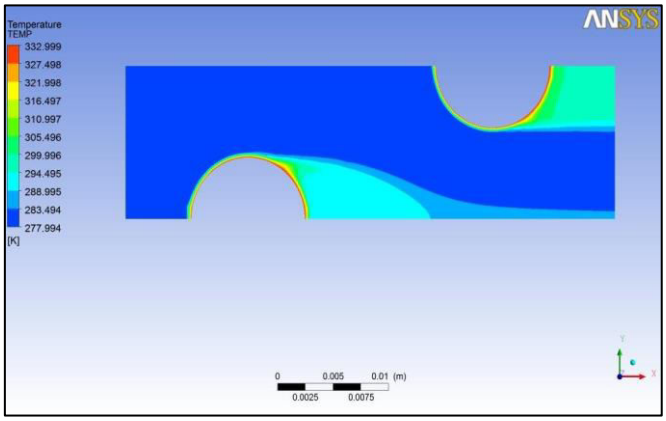

Figure 3.6 Contour of Temperature for inlet velocity 6.2 m/s, SST k-omega flow model

Comparison of Numerical and Experimental Results

For ten inflow velocities, data on pressure drop, maximum velocity, and heat transfer coefficient are recorded. Friction factor and Coburn j-factor are derived using these recorded values. To compare with experimental data, the Fanning friction factor f is listed in Table 3.3 and plotted against Reynolds number in Figure 3.7. The graph (Figure 3.7) shows that simulated and experimental values follow the same trend. Figure 3.8 depicts the % error in simulated values compared to experimental friction factor f values.

|e-ISSN: 2319-8753, p-ISSN: 2320-6710| www.ijirset.com | Impact Factor: 8.423| A Monthly Peer Reviewed & Referred Journal |

|| Volume 12, Issue 7, July 2023 ||

| DOI:10.15680/IJIRSET.2023.12070010|

Table 3.3 Fanning friction factor f (Numerical Results)

Re	Fanning friction factor f (Numerical Results)		
	Laminar	k-epsilon	SST k-omega
330	0.114301	0.12834	0.11573
600	0.078958	0.085486	0.08113
790	0.063243	0.066578	0.066373
1300	0.049123	0.048782	0.053733
1700	0.042439	0.040209	0.046074
2900	0.033973	0.030271	0.034262
4300	0.028998	0.02524	0.028268
5200	0.027105	0.023353	0.02569
6200	0.025445	0.022123	0.02361
7200	0.024416	0.021219	0.022234

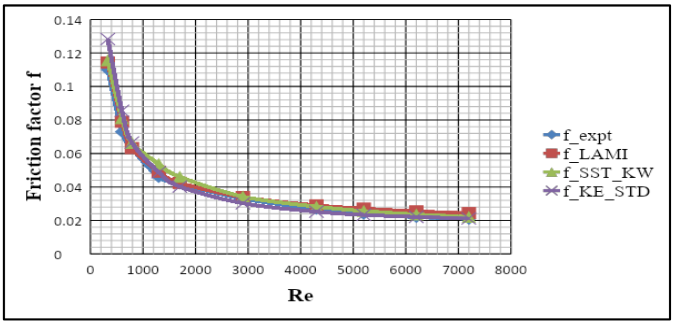

Fig 3.7 Comparison of experimental and numerical values for friction factor f

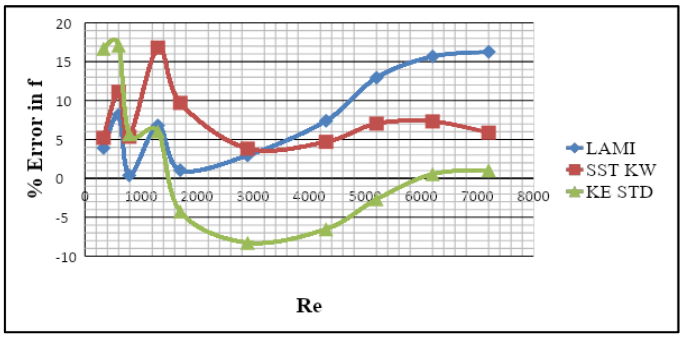

Fig 3.8 Percentage error in friction factor f

The Coburn j-factor is tabulated and compared to the experimental value in the same way. Finally, the % error for simulated values against experimental values is presented.

Table 3.4 Colburn j-factor (Numerical Results)

Re	Colburn j factor (Numerical Result)		
	Laminar	k-epsilon	SST k-omega
330	0.034964	0.039524	0.035225
600	0.027451	0.032419	0.027989
790	0.023432	0.027021	0.02414
1300	0.018764	0.021256	0.020222
1700	0.015851	0.017826	0.017801
2900	0.01165	0.012691	0.013595
4300	0.00879	0.009822	0.010913
5200	0.00784	0.008457	0.009719
6200	0.006792	0.007277	0.008869
7200	0.00596	0.006512	0.007978

|e-ISSN: 2319-8753, p-ISSN: 2320-6710| www.ijirset.com | Impact Factor: 8.423| A Monthly Peer Reviewed & Referred Journal |

|| Volume 12, Issue 7, July 2023 ||

| DOI:10.15680/IJIRSET.2023.12070010|

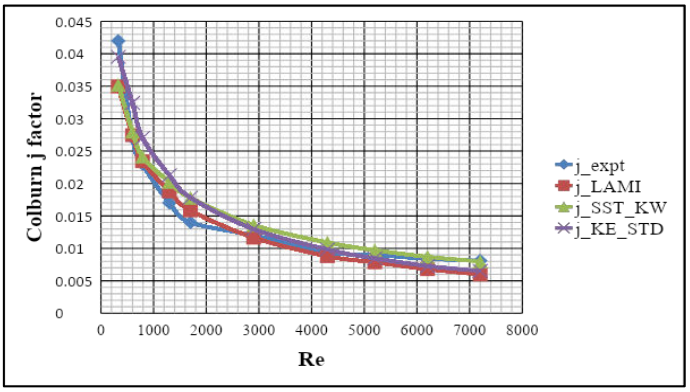

Fig 3.9 Comparison of experimental and numerical values for Colburn j-factor

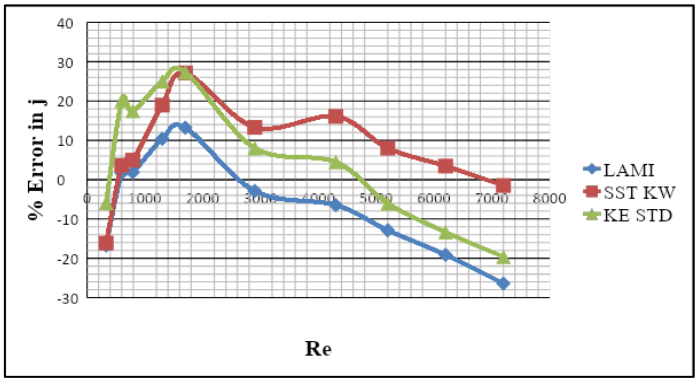

Fig 3.10 Percentage error in Colburn j-factor

The simulation results for the different flow models were used to calculate the heat transfer characterization parameter Colburn j-factor. At different Reynolds numbers, the flow models reveal extremely clear differences in their ability to replicate heat transfer. The laminar flow model, as expected, is the best for forecasting the j-factor in laminar flow. A laminar and k-epsilon turbulence model is excellent for describing transition heat flow, whereas the k-omega model is best for calculating turbulent heat flow.

IV. CONCLUSION AND FUTURE SCOPE

Conclusion

The objective of this project is to develop the CFD simulation model for two-row fin-and-tube heat exchanger and verify the results of simulation with the available experimental data from the literature. The purpose of the work was to investigate the possibilities of eventually using CFD calculations for design of heat exchangers instead of expensive experimental testing and prototype production.

To analyse the flow and heat transfer characteristics of the heat exchanger, a model of a two-row fin-and-tube heat exchanger is created using Design modeller and Mesh module to create the geometry and mesh respectively. The resulting mesh (after a grid independence test was carried out) is used for running simulations using a laminar flow model and two turbulence models. Ten different inlet flow velocities ranging from 0.3 m/s to 6.2 m/s and corresponding to Reynolds numbers ranging from 330 to 7200 are simulated in the three different flow models (laminar, k-epsilon turbulence model, and SST k-omega turbulence model). Using the simulation results calculations related to heat flow and pressure loss are carried out to determine the Fanning friction factor f and Colburn j-factor for comparison with the literature values used for the validation.

It is found that the flow model accuracy depended on the flow regime and whether the friction factor f or j-factor is being determined. From the experimental values given in the literature, the laminar flow region for this particular geometry of heat exchanger switched to transitional at around Reynolds number 1300, and moving to turbulent around Reynolds number 2900. The Reynolds number has a characteristic dimension of the tube collar outside diameter.

|e-ISSN: 2319-8753, p-ISSN: 2320-6710| www.ijirset.com | Impact Factor: 8.423| A Monthly Peer Reviewed & Referred Journal |

|| Volume 12, Issue 7, July 2023 ||

| DOI:10.15680/IJIRSET.2023.12070010|

REFERENCES

1. Yuzhu Zhou, Lin Zhang, Shi Bu, Cheng Sun, Weigang Xu, Yongchang Xiao and Lin Liu, [Study on Heat Transfer Characteristics of the Whole Plate Fin Tube Cooler], International Journal of Thermofluid Science and Technology (2020) Volume 7, Issue 2, Paper No. 070204.
2. Subodh Bahirat and P. V. Joshi, [CFD Analysis of Plate Fin Tube Heat Exchanger for Various Fin Inclinations], Subodh Bahirat Int. Journal of Engineering Research and Applications, ISSN : 2248-9622, Vol. 4, Issue 8(Version 3), August 2014, pp.116-125.
3. M. Shawky Ismail, M. Hassab and Wael M. El-Maghlany, [Comparative Three Dimensional CFD Study for Inline Cross Flow Plate Finned Tube Heat Exchanger], Proceedings of the 4 th World Congress on Momentum, Heat and Mass Transfer (MHMT'19) Rome, Italy – April, 2019.
4. Ishwar J.Dhangar and Dr. Manojkumar Chopra, [Experimental Investigation and CFD Analysis Performance of Fin and Tube Heat Exchanger with Different Types of Fins], International Journal of Engineering Research & Technology (IJERT) ISSN: 2278-0181. Special Issue - 2017.
5. K. Ranjithkumar, M. Santhoshkumar and R. Periyasamy, [Experimental and Numerical Analysis of Heat Transfer on Plate Fin Heat Exchanger at Different Fin Pitches with Ceramic Coating], International Journal of Engineering Research & Technology (IJERT) ISSN: 2278-0181 Published by, www.ijert.org ICITMSEE - 2018 Conference Proceedings.
6. Mladen Bošnjakovi´c and and Simon Muhi˘c, [Numerical Analysis of Tube Heat Exchanger with Perforated Star-Shaped Fins], Fluids 2020, 5, 242.
7. Yuvraj Singh Rajput and Abhishek Arya, [CFD Analysis of Cross Flow Heat Exchanger with Different Fin Thickness], International Journal Of Innovative Research In Technology, July 2019 | IJIRT | Volume 6 Issue 2 | ISSN: 2349-6002.
8. Abhishek Mishra and Dr. Nitin Tenguria, [Experimental Investigation of Heat Transfer in Modified Finned Tube Banks Arrangement with in-Line and Staggered Layout], International Journal Of Innovative Research In Technology, August 2020| IJIRT | Volume 7 Issue 3 | ISSN: 2349-6002.
9. Arafat Ahmed Bhuiyan and A K M Sadrul Islam, [CFD analysis of different Fin-and-Tube Heat Exchangers], Proceedings of the 13th Annual Paper Meet 25 September 2010, Dhaka.
10. Young-Chang Liu, Somchai Wongwises, Wen-Jeng Chang and Chi-Chuan Wang, [Airside performance of fin-and-tube heat exchangers in dehumidifying conditions – Data with larger diameter], International Journal of Heat and Mass Transfer 53 (2010) 1603–1608.
11. Wenxiao Chu, Pengqing Yu, Ting Ma, Min Zeng and Qiuwang Wang, [Numerical Analysis of Plain Fin-and-Oval-Tube Heat Exchanger with Different Inlet Angles], Chemical Engineering Transactions, VOL. 35, 2013.
12. Shubham Gupta and Karan Singh Verma, [Computational Fluid Dynamics Analysis Of Shell And Tube Heat Exchanger With Having Different Types Of Fins], International Journal for Research Trends and Innovation, 2022 IJRTI | Volume 7, Issue 2 | ISSN: 2456-3315.

INNO SPACE
SJIF Scientific Journal Impact Factor

Impact Factor: 8.423

doi cross ref

ISSN INTERNATIONAL STANDARD SERIAL NUMBER INDIA

निस्केयर NISCAIR

INTERNATIONAL JOURNAL OF INNOVATIVE RESEARCH

IN SCIENCE | ENGINEERING | TECHNOLOGY

9940 572 462 6381 907 438 ijirset@gmail.com

Scan to save the contact details